

1 **Biomechanics of Two External Fixator Devices Used in Rat Femoral Fractures**

2 Liza Osagie-Clouard¹, Joshua Kaufmann¹, Gordon Blunn^{1,2}, Melanie Coathup³, Catherine Pendegrass¹,
3 Richard Meeson¹, Timothy Briggs⁴, Mehran Moazen⁵

4 ¹Division of Surgery, University College London, Stanmore, UK; ²University of Portsmouth,
5 Portsmouth, UK; ³University of Central Florida, USA; ⁴Royal National Orthopaedic Hospital,
6 Stanmore, UK; ⁵Mechanical Engineering, University College London

7
8 Corresponding Author

9 Liza Osagie-Clouard

10 IOMS,

11 Royal National Orthopaedic Hospital

12 Brockley Hill

13 Stanmore HA7 4LP

14 +447931809218

15 l.osagie@ucl.ac.uk

16
17 Running title: external fixator biomechanics, and FEA

18
19 Author contributions: LOC, manuscript preparation, data collection, experimental design. JK

20 experimental design, data collection. GB, experimental design, manuscript preparation.

21 MC/CP/TB, experimental design and data analysis. RM, computational modelling and

22 manuscript preparation. MM, experimental design, data analysis, manuscript preparation.

23 all authors have read and approved the final submitted manuscript

27 **Abstract**

28 The use of external fixators allows for the direct investigation of newly formed
29 interfragmentary bone, and the radiographic evaluation of the fracture. We validated the
30 results of a finite element model with the in vitro stiffness' of two widely used external fixator
31 devices used for in vivo analysis of fracture healing in rat femoral fractures with differing
32 construction (Ti alloy ExFix1 and PEEK ExFix2).

33

34 Rat femoral fracture fixation was modelled using two external fixators. For both constructs an
35 osteotomy of 2.75 mm was used, and offset maintained at 5 mm. Tufnol, served as
36 standardized substitutes for rat femora. Constructs were loaded under axial compression
37 and torsion. Overall axial and torsional stiffness were compared between the in vitro models
38 and FE results. FE models were also used to compare the fracture movement and overall
39 pattern of von Mises stress across the external fixators.

40

41 In vitro axial stiffness of ExFix1 was $29.26 \text{ N/mm} \pm 3.83$ compared to ExFix2 $6.31 \text{ N/mm} \pm$
42 0.67 ($p^* < 0.05$). Torsional stiffness of ExFix1 was $47.5 \text{ Nmm}^0 \pm 2.71$ compared to ExFix2 at
43 $19.1 \text{ Nmm}^0 \pm 1.18$ ($p^* < 0.05$). FE results predicted similar comparative ratios between the
44 ExFix1 and 2 as the in vitro studies. FE results predicted considerably larger
45 interfragmentary motion in the ExFix2 comparing to ExFix1.

46

47 We demonstrated significant differences in the stiffness' of the two external fixators as one
48 would expect from such variable designs; yet, importantly we validated the utility of an FE
49 model for the analysis and prediction of changes in fracture mechanics dependent on fixator
50 choice.

51

52 Keywords: fracture fixation, finite element analysis, biomechanics

53

54

55 **1. Introduction**

56 Multiple physiological and mechanical factors govern the fracture healing process. Overall
57 stiffness of the fracture fixation construct directly impacts the axial, torsional and shear
58 interfragmentary movement at the fracture site (1-3). These subsequently impact the healing
59 process and as with physiological healing, rigid fixation will lead to intramembranous
60 ossification, while those that are less rigid, allow for the creation of cartilaginous callus and
61 endochondral ossification (4, 5).

62 Rodents have been widely used to investigate the fracture fixation. They are an invaluable
63 animal model used to understand the fracture healing process and to develop new
64 technologies and treatments to address complications such as non-union. A number of
65 external fixators have been used to fix femoral fractures in rodents. These fixators, typically
66 result in a combination of intramembranous and endochondral ossification with studies
67 illustrating healing by various biological scenarios in different models (6, 7).

68 The literature comparing the biomechanical differences of existing external fixators in
69 rodents is limited. Harrison et al. (8) reported no significant difference in axial stiffness
70 between aluminium and titanium fixator bar materials. However, pin material and thickness
71 does have a large effect on torsional and axial stiffness. Mark et al. (9) reported a 50%
72 decrease in axial stiffness and transverse stiffness of the fixator, when using a 1.0-mm
73 compared to a 1.2-mm outer diameter pin. Willie et al. (10) demonstrated significantly
74 reduced stiffness at the fracture site of titanium alloy pins versus stainless steel in fixators of
75 the same design, with similar effects of body material and offset on stiffness as previous
76 studies. Glatt et al. (11) reported the development of a variable stiffness PEEK fixator where
77 fracture rigidity can be altered during healing. This PEEK fixator is gaining favour for use in
78 the investigation of rodent fracture healing as the four pin construct is lighter than traditional
79 titanium and stainless steel fixators and has been shown to be well tolerated in vivo (12). In
80 contrast, the majority of studies utilise a more traditional unilateral fixator design such as the

81 Harrison et al. titanium alloy fixator. Recently reported variations of the Harrison fixator utilise
82 2 carbon fibre cross bars with four aluminium pins (13, 14); heavier than the Glatt fixator.
83 Therefore, while there is a body of literature on the biomechanics of different external
84 fixators on rodents (see also 15,16) and some variations of them e.g. their material
85 properties and dimensions, to best of our knowledge, no study has compared the effects of a
86 variable stiffness fixator and a static fixator on the in vitro stabilisation of a rat femoral
87 fracture model. These are two different external fixator designs and a direct biomechanical
88 comparison between them lacks in literature and is crucial to advance our understanding of
89 the interplay between the biomechanical and biological factors in the context of fracture
90 healing.

91 Studies investigating the effect of fixator construct on fracture stabilisation can be laborious,
92 necessitating investigation of each design parameter-including crossbar number/size/ offset,
93 pin size and each component material. Subsequently, the ability to utilise computational
94 modelling to determine the mechanical characteristics of any fixator construct, is invaluable.
95 So long as the models are validated using in vivo or in vitro experimental data finite element
96 (FE) modelling provides a unique opportunity to model experimental scenarios
97 computationally and accurately (17-19). As such, the creation of a validated design tool, that
98 can replicate in vivo biomechanics, allow the augmentation and refinement of fixator
99 characteristics to best suit experimental conditions, and yet does so in a timely and cost
100 effective fashion-would be most beneficial to those working with fracture experimental
101 models.

102 The aim of this study was to compare the biomechanics of two increasingly utilised rodent
103 external fixators; a derivation of the Harrison et al titanium alloy fixator, and the Glatt/AO
104 PEEK external fixator, but more importantly to validate an FEA model of design with the ex
105 vivo data. These fixators where chosen specifically in order to attempt FEA validation with
106 two very disparate fixator designs. We utilised a series of experimental in vitro testing and in
107 silico computational models based on finite element method.

108 **2. Materials and Methods**

109 **2.1 External fixator designs**

110 The study compared two external fixator designs. The first (ExFix1) has two graphite cross
111 bars of 2x40 mm, spaced 4 mm apart, fixed between two titanium alloy (Ti6Al-4v) blocks.
112 These blocks measured 8mm in height, 10 mm in width and 7.2 mm in depth. This design
113 used 4 titanium alloy threaded pins of 0.8/1.0 mm, fixed within the blocks with stainless steel
114 grub screws. The second fixator (ExFix2) was comprised of a single PEEK crossbar and
115 again four stainless steel threaded pins. The crossbar measured 16.5 mm long, 5 mm wide
116 and 2 mm deep with four 1mm holes to locate the steel pins. A single 12.5 mm long, 1 mm
117 wide rectangular opening runs parallel with the openings for the steel pins; again each pin
118 measured 0.8/1.0 mm. The offset as measured from the free length of the pins beneath the
119 crossbar to the upper surface of the bone, was kept constant at 5 mm throughout testing.
120 ExFix1 weighed 6.23 g (range 6.22-6.31 g), and ExFix 2 3.11 g (range 3.08-3.65 g).

121 A hollowed homogenous rod of laminated Tufnol (Tufnol Composites, Birmingham, UK), of
122 similar elastic modulus to adolescent rat femora (inner diameter 1.5 mm, outer diameter 4
123 mm, length 35 mm) served as standardised substitute for bone and fixed using ExFix1 (n=5)
124 and 2 (n=5). Fixation was carried out using custom drill guides of 0.8 mm that allowed for the
125 accurate predrilling of holes into the Tufnol, after which pins were manually screwed into
126 position to breach both cortices by one thread. After the fixator was fixed to the Tufnol bone
127 a fracture was created with a 2.75 mm fracture gap maintained.

128 **2.2 In vitro testing**

129 The Tufnol specimens were tested non-destructively using a Zwick (Zwick-Roell, Germany)
130 materials testing machine to determine axial and torsional stiffness. In compression, a
131 maximum load of 40 N was applied, with a preload of 0.5 N at a rate of 0.5 mm/min. Load
132 was applied onto potted concave ends of the Tufnol via steel beads attached to the testing
133 machine, and the loading-unloading process repeated three times for each sample.

134 In torsion both ends of the sample were fixed into titanium cylinders with grub screws to
135 negate slipping during testing. One end of the Tufnol remained static, whilst a maximum
136 vertical load of 40 N was applied to the other end with a lever arm of 75 mm, which led to
137 torsion of 3000 Nmm. Loading was repeated three times per specimen and torsional
138 stiffness was calculated by dividing the applied torque by the degrees of rotation of the
139 proximal end of the Tufnol.

140 **2.3 Finite element analysis**

141 Computer-aided design models of the bone and two external fixators were developed in
142 CATIA V5 (Dassault Systèmes, Paris FR - Figure 1). Dimensions exactly reflected those of
143 the real-life fixator models and all parts assigned isotropic material properties; The Tufnol
144 bone model has an elastic modulus of 6.5 GPa and Poisson's ratio 0.4 (20-22). Titanium
145 alloy blocks in the ExFix1 have an elastic modulus of 96 GPa and a Poisson's ratio of 0.36.
146 The Graphite rods have an elastic modulus of 4.1 GPa and a Poisson's ratio of 0.17. The
147 PEEK crossbar of the ExFix2 has an elastic modulus of 3.6 GPa and a Poisson's ratio of
148 0.38. Finally, stainless steel pins in both fixators were given the same mechanical properties:
149 an elastic modulus of 193 GPa and Poisson's ratio of 0.31. The effect of screw pull-out at the
150 fixator-Tufnol interface was ameliorated by gluing these contacts during experimental
151 testing; subsequently, the interface experienced minimal micro-motion upon loading in-vitro
152 and allowed all pin-Tufnol interfaces to be modelled as "fully fixed".

153 Interfaces such as at the crossbar-pin interface had inherent micro-motion as they were
154 either threaded into position or held with grub screws. Thus two simulations were created,
155 one with all contacts "fully fixed" and a second with all grub screws and threaded contacts
156 "relaxed" to account for this motion. The relaxed model used contact elements at the
157 interfaces with a friction coefficient of 0.4 (17). The expectation being that the properties of
158 each fixator would be between these two extreme models.

159 In order to replicate the boundary conditions of the test rigs, the constraints were applied
160 within the concave housing of the Tufnol under axial loading conditions and along the
161 outside face of the housing under torsional loading conditions. Additionally, the surface/node
162 in which the load was applied was also constrained to translate in only the axis parallel to the
163 line of loading.

164 Analyses were carried out in FE package ANSYS (Academic Research, Pennsylvania USA).
165 Tetrahedral elements were used to mesh all components of the fixators and Tufnol.
166 Convergence was tested on each fixator by increasing the number of elements from ca.
167 5,000 to 2,000,000 incrementally. The solution for ExFix1 converged to within 5% at
168 approximately 135,000 elements when measuring axial stiffness and approximately 260,000
169 elements when measuring torsional stiffness. For ExFix2, the solution converged for both
170 quantities of interest at approximately 322,000 elements. Results converged substantially
171 faster with the use of mid-side nodes, and as such they were used throughout.

172 In addition to axial and torsional stiffness, FEA was also used to evaluate fracture gap
173 displacement as measured by nodes either side of the osteotomy. Von Mises stresses were
174 calculated for each fixator and the points of maximal stress also determined. It must be
175 noted that since in this study no detail validation of the strain pattern was carried out the
176 stress results were analysed qualitatively.

177 **2.4 Statistical Analysis**

178 Statistical analysis was performed on the experimental data. The ANOVA assumption of
179 normality was tested using the Shapiro–Wilks normality test. If the assumption was met, an
180 ANOVA was performed, if not, a Mann Whitney *U* test was used. The data was analysed
181 using Prism 4.03 (GraphPad Software Inc., San Diego, USA) and a significance level when
182 comparing data was set at $p < 0.05$.

183 **3. Results**

184 **3.1 Axial stiffness:**

185 ExFix1 was 29.26 N/mm \pm 3.83 compared to ExFix2 6.31N/mm \pm 0.67 ($p^* < 0.05$). The fully
186 restricted FEA model predicted axial values of 79.95N/mm and 31.57N/mm for ExFix1 and 2
187 respectively. The model under secondary contact conditions produced axial values of 46.12
188 N/mm and 7.52 N/mm respectively (Figure 2A).

189

190 **3.2 Torsional stiffness:**

191 ExFix1 was 47.5 Nmm/ $^{\circ}$ \pm 2.71 compared to ExFix 2 at 19.1 Nmm/ $^{\circ}$ \pm 1.18 ($p^* < 0.05$). The
192 fully restricted FEA model predicted torsional stiffness of 98 Nmm/ $^{\circ}$ and 50 Nmm/ $^{\circ}$ for ExFix1
193 and 2 respectively. The model under secondary contact conditions produced torsional
194 stiffness of 89.8 Nmm/ $^{\circ}$ and 27 Nmm/ $^{\circ}$ respectively (Figure 2B).

195

196 **3.3 Comparative ratios:**

197 The ratio of ExFix1: ExFix2, axial and torsional stiffness based on the in vitro experimental
198 data was 4.6 and 2.5 respectively. The same ratio based on the FEA with fully fixed interface
199 conditions were 2.5 (46% lower than the experimental data) and 2 (20% lower than the
200 experimental data) for the axial and torsional stiffness respectively. The same ratio based
201 on the FEA with relaxed interface were 5.1 (11% greater than experimental data) and 3.3
202 (32% greater than experimental data) for the axial and torsional stiffness respectively (Figure
203 3).

204

205 **3.4 Fracture movement:**

206 Total fracture movement as measured in the FE models, was greater for ExFix2 in all planes
207 versus ExFix1. Less than 1mm of movement occurred with ExFix1 at the maximal loading
208 however, in the ExFix2 the fragments come into contact leading to a fracture movement of
209 about 2.7 mm based on the relaxed interface model. Under axial loading ExFix1 was found

210 to have 0.54 and 0.91 mm of movement with the fully fixed and relaxed models. Whereas
211 ExFix2 demonstrated 1.49 and 2.75 mm of movement respectively. Under torsional
212 conditions, ExFix1 showed 0.52 and 0.64 mm of movement with the fully fixed and relaxed
213 models. Versus ExFix2 with 2.20 and 2.74 mm of movement respectively (Figure 4A and b).

214

215 **3.5 Stress pattern:**

216 The stress contour plots of the equivalent von Mises stresses for each fixator component are
217 shown in Figure 5. In all components of the fixator ExFix1 experienced lower overall stress
218 than ExFix2, in both axial and torsional loading. For all FE analysis maximum stress
219 occurred at the pin-Tufnol interface. In axial loading of both fixators, stress peaks in the pin
220 closest to the point of loading was seen, whilst in torsion, maximum stress occurred in the
221 pins either side of the fracture gap.

222 **4. Discussion**

223 This study compared the mechanical characteristics of two commonly used external fixators
224 in small animal fracture models. We used our in vitro findings to validate a series of finite
225 element models based on axial and torsional stiffness data. Between the two fixators, we
226 found significant differences in stiffness in both the axial and rotational planes, with ExFix1
227 markedly more rigid in both planes. Throughout the study we maintained a constant offset,
228 pin material and pin diameter, thus allowing the fixator design and crossbar material (Ti
229 alloy/carbon fibre vs. PEEK) to be the dominating factors on overall stiffness. Previous
230 studies have determined that pin size and material are the greatest determinants of fixator
231 stiffness and interfragmentary fracture movement, also demonstrating the importance of
232 offset and pin number (10, 23, 24), our data also suggests the significant impact that the
233 fixator material properties and bar configuration have on the overall stiffness.

234 In vitro axial stiffness of both ExFix constructs were significantly less than those found with
235 locked nailing techniques (25). ExFix1 was a third as stiff, and ExFix2 just over half as stiff

236 as reported nailing data (25). Conversely rotational stiffness was greater for the external
237 fixators than locked intramedullary nails, and indeed was greater than physiological numbers
238 from intact bone (torsional stiffness 23 Nmm/°). This greater stiffness in rotation, if related in
239 vivo, will lead to reduced interfragmentary movement in shear and as such will impact bone
240 formation.

241 Our data suggests the FE model could predict the relative differences between the two
242 external fixators. However, the FE models consistently predicted larger stiffness' then those
243 found in vitro, this difference was considerably larger in the "fixed" model that did not
244 account for any micro-motion at the pin-Tufnol or the pin-fixator interfaces. When relaxing
245 the interfaces, the comparative ratios fell notably and were closer to the experimental in vitro
246 data (see Figure 2). Again highlighting the fundamental role of micromotion at the interfaces
247 in both the in silico and in vitro tests (17).

248 A relatively large body of work has evaluated the role of FE modelling in clinical fracture
249 fixation scenarios. For example, Ramlee et al. (26) reviewed two external fixators with an FE
250 model and their effects on subtalar dislocation reduction, similarly, Varga et al. (27) reviewed
251 the use of compression screws in scaphoid fracture fixation and the effects these have on
252 interfragmentary forces and again fracture reduction. Both of these studies amongst others
253 (e.g. 3, 28) have validated FE models and underlined their utility in clinical fracture
254 management. Our study uses the modelling technique in the preclinical setting; importantly
255 allowing an understanding of the fracture mechanics without the need for lengthy in vivo
256 experiments. Moreover, the validation of our relaxed FE model, that adjusts for interface
257 micro motion, results in the creation of a tool that can allow the design and manipulation of a
258 fixator to best suit different experimental parameters.

259 The difference in stiffness has a predictable effect on movement at the fracture gap, which
260 has important implications on fracture healing. Interfragmentary motion of between 0.2-1 mm
261 perpendicular to a diaphyseal fracture has been found to promote union; however, excessive

262 axial and shear motion will result in delayed healing (1-3). Under axial conditions ExFix2
263 experiences significant motion where bony fragments come into contact. ExFix1, however,
264 restricts vertical motion under axial loading to less than 1 mm, within the desired envelope.
265 Under torsion, this increases to a value equating to a rotation of up to 17 degrees. ExFix1
266 limits rotation to less than half this amount at the same levels of loading. Under axial loading,
267 translation and rotation at the fracture gap in ExFix1 is also negligible. Additionally, our
268 findings are particularly relevant when investigating biological and pharmacological
269 interventions where variability in stress across the gap will directly influence the efficacy of
270 these factors (29-31).

271 The specific pin where the maximum stress occurs changes between loading conditions. In
272 axial loading, maximum stress is located on the most proximal pin in both ExFix1 and ExFix2
273 whereas under torsion, maximum stress occurred in the pin nearest the proximal end of the
274 fracture. These changes are likely to be a function of the constraint of the Tufnol bone
275 creating higher stresses in the pins adjacent to the fracture site.

276 While the FE model could not exactly represent the in vitro assembly boundary conditions,
277 the two conditions that were investigated can accurately predict upper and lower limits for in
278 vitro results. Ultimately, we demonstrated considerable differences in the overall stiffness
279 between the two fixators, which should be considered when comparing experimental *in vivo*
280 data on fracture healing. Given a consistent fracture gap fractures stabilised using ExFix2
281 are more likely to heal through endochondral ossification or go onto a delayed or non-union
282 compared to ExFix1. The in silico model where the threads are not fully bonded, predicted
283 the comparative stiffness between the two fixators, as evidenced by the similar ratios. This
284 data suggests that a computational protocol that includes the micro-motion present at the
285 pin-bone interface, results in a reproducible model of experimental conditions. Further in vivo
286 and computational work is required to demonstrate the effect of gap distance and fixator
287 stiffness on the rate, type and quality of ossification and healing.

288

289 **Acknowledgments**

290 Funding was obtained from The Rosetrees and Gwen Fish Orthopaedic Trusts. Moazen was
291 supported by Royal Academy of Engineering Research Fellowship.

292 **References**

293 1. Goodship AE, Kenwright J. The influence of induced micromovement upon the healing of
294 experimental tibial fractures. *J Bone Joint Surg Br.* 1985;67,650–655.

295 2. Claes LE, Heigele CA, Neidlinger-Wilke C, Kaspar D, Seidl W, Margevicius KJ, Augat P.
296 Effects of mechanical factors on the fracture healing process. *Clin Orthop Relat Res.*
297 1998;355,S132–147.

298 3. Moazen M, Jones AC, Leonidou A, Jin Z, Wilcox RK, Tsiridis E. Rigid versus flexible plate
299 fixation for periprosthetic femoral fracture - computer modelling of a clinical case. *Medical*
300 *Engineering & Physics* 2012;34,1041-1048.

301 4. McKibbin B. The biology of fracture healing in long bones. *J Bone Joint Surg.* 1978;60-
302 B,150–162.

303 5. Mark H, Nilsson A, Nannmark U, Rydevik B. Effects of fracture fixation stability on
304 ossification in healing fractures. *Clin Orthop Relat Res.* 2004;419,245-50.

305 6. Histing T, Garcia P, Holstein JH, Klein M, Matthys R, Nuetzi R, Steck R, Laschke MW,
306 Wehner T, Bindl R, Recknagel S, Stuermer EK, Vollmar B, Wildemann B, Lienau J, Willie B,
307 Peters A, Ignatius A, Pohlemann T, Claes L, Menger MD. Small animal bone healing
308 models: standards, tips, and pitfalls results of a consensus meeting. *Bone.* 2011;49,591-599.

- 309 7. Holstein JH, Garcia P, Histing T, Kristen A, Scheuer C, Menger MD, Pohlemann T.
310 Advances in the establishment of defined mouse models for the study of fracture healing and
311 bone regeneration. *J Orthop Trauma*. 2009;23,S31-8.
- 312 8. Harrison LJ, Cunningham JL, Strömberg L, Goodship AE. Controlled induction of a
313 pseudoarthrosis: a study using a rodent model. *J Orthop Trauma*. 2003;17,11-21.
- 314 9. Mark H, Bergholm J, Nilsson A. An external fixation method and device to study fracture
315 healing in rats. *Acta Orthop Scand* 2003;74,476–482.
- 316 10. Willie B, Adkins K, Zheng X. Mechanical characterization of external fixator stiffness for a
317 rat femoral fracture model. *J Orthop Res* 2009;27,687–693.
- 318 11. Glatt V, Evans C, Matthys R. Design, characterisation and in vivo testing of a new,
319 adjustable stiffness, external fixator for the rat femur. *European Cells and Materials*. 2012;
320 12,289-299.
- 321 12. Glatt V, Bartnikowski N, Quirk N, Schuetz M, Evans C. Reverse Dynamization: Influence
322 of Fixator Stiffness on the Mode and Efficiency of Large-Bone-Defect Healing at Different
323 Doses of rhBMP-2. *J Bone Joint Surg Am*. 2016;98,677-87.
- 324 13. Ho CY, Sanghani A, Hua J, Coathup M, Blunn G. Mesenchymal stem cells with
325 increased stromal derived factor 1 expression enhance fracture healing. *Tissue Eng Part A*.
326 2015;21, 594-602.
- 327 14. Lee O, Coathup M, Gooip A, Blunn G. Use of mesenchymal stem cells to facilitate bone
328 regeneration in normal and chemotherapy treated rats. *Tissue Eng*. 2005;11,1727-1735.
- 329 15. Kaspar K, Schell H, Toben D, Matziolis G, Bail HJ. An easily reproducible and
330 biomechanically standardized model to investigate bone healing in rats, using external
331 fixation. *Biomed Tech*. 2007;52,383-390.

- 332 16. Strube P, Mehta M, Putzier M, Matziolis G, Perka C, Duda GN. A new device to control
333 mechanical environment in bone defect healing in rats. *J Biomech.* 2008;41,2696-2702.
- 334 17. Moazen M, Mak J, Jones AC et al. Evaluation of a new approach for modelling the
335 screw-bone interface in a locking plate fixation: a corroboration study. *J Eng in Med Part H.*
336 2013; 227(7),746-756.
- 337 18. Macleod A, Panka P, Simpson A. Does screw-bone interface modelling matter in finite
338 element analyses? *J Biomech.* 2012;45,1712-1716.
- 339 19. Wieding J, Souffrant R, Fritsche A. Finite element analysis of osteosynthesis screw
340 fixation in the bone stock: An appropriate method for automatic screw modelling. *PLoS One.*
341 2012;7,1371.
- 342 20. Tufnol Composites Limited. 2016. Carp Brand Tufnol [online]:
343 http://www.tufnol.com/materials-full/fabric_laminates/carp-brand.aspx
- 344 21. ANSYS® Academic Research, Release 16.2. Engineering data, material properties,
345 ANSYS, Inc.
- 346 22. AZO Materials. No date available. Supplier Data - Polyetheretherketone (PEEK)
347 (Goodfellow) and Carbon - Graphite Materials [online].
- 348 23. Mark H, Nilsson A, Nannmark U. Effects of fracture fixation stability on ossification in
349 healing fractures. *Clin Orthop Relat Res* 2004 419:245–250.
- 350 24. Mark H, Rydevik B. Torsional stiffness in healing fractures: influence of ossification: an
351 experimental study in rats. *Acta Orthop* 2005;76,428–433.
- 352 25. Schoen M, Rotter R, Schattner S. Introduction of a new interlocked intramedullary nailing
353 device for stabilization of critically sized femoral defects in the rat. *J Orthop Res* 2008;
354 26,184–189.

355

356 26. Ramlee MH, Kadir MR, Murali MR, Kamarul T. Biomechanical evaluation of two
357 commonly used external fixators in the treatment of open subtalar dislocation-a finite
358 element analysis. *Med Eng Phys.* 2014;36,1358-1366.

359 27. Varga P, Zysset PK, Schefzig P, Unger E, Mayr W, Erhart J. A finite element analysis of
360 two novel screw designs for scaphoid waist fractures. *Med Eng Phys.* 2016;38,131-139.

361 28. Wang Y, Wong DW, Zhang M. Computational models of the foot and ankle for
362 pathomechanics and clinical applications: a review. *Ann Biomed Eng.* 2016 Jan;44(1),213-
363 221.

364 29. Sato M, Yasui N, Nakase T, Kawahata H, Sugimoto M, Hirota S, Kitamura Y, Nomura S,
365 Ochi T. Expression of bone matrix proteins mRNA during distraction osteogenesis. *J Bone*
366 *Miner Res* 1998;13,1221-1231.

367 30. Sato M, Ochi T, Nakase T, Hirota S, Kitamura Y, Nomura S, Yasui N. Mechanical
368 tension-stress induces expression of bone morphogenetic protein (BMP)- 2 and BMP-4, but
369 not BMP-6, BMP-7, and GDF-5 mRNA, during distraction osteogenesis. *J Bone Miner Res*
370 1999;14,1084-1095.

371 31. Seebach C, Skripitz R, Andreassen TT, Aspenberg P. Intermittent parathyroid hormone
372 (1-34) enhances mechanical strength and density of new bone after distraction osteogenesis
373 in rats. *J Orthop Res* 2004;22,472-478.

374

375 **Figure Legends**

376 Figure 1. Computer aided designs of both external fixator models, with arrows demonstrating
377 load constraint conditions.

378 Figure 2A and B. Demonstrating the torsional and axial stiffness' of both external fixators in
379 vitro and in silico.

380 Figure 3. Demonstrating the comparative stiffness ratios in torsion and compression for in
381 vitro and in silico testing.

382 Figure 4A and B. Demonstrating total fracture movement as found in silico under
383 compression (A) and torsion (B).

384 Figure 5. Equivalent von-Mises stress contour plots on the crossbars of both fixator models.

385

386

387

388

389

390

391

392

393

394

395

396

397

398 Fig 1

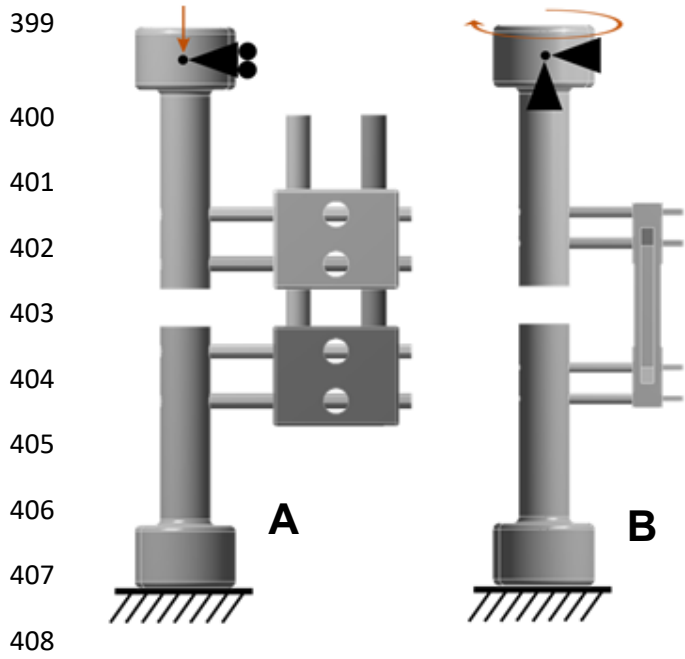
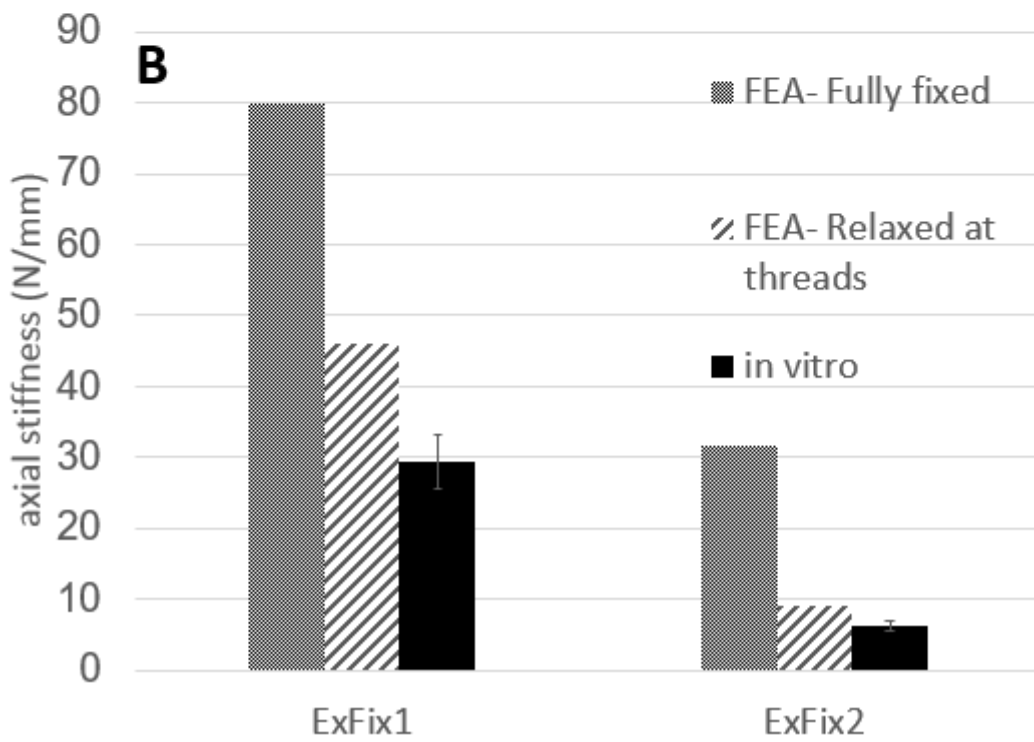
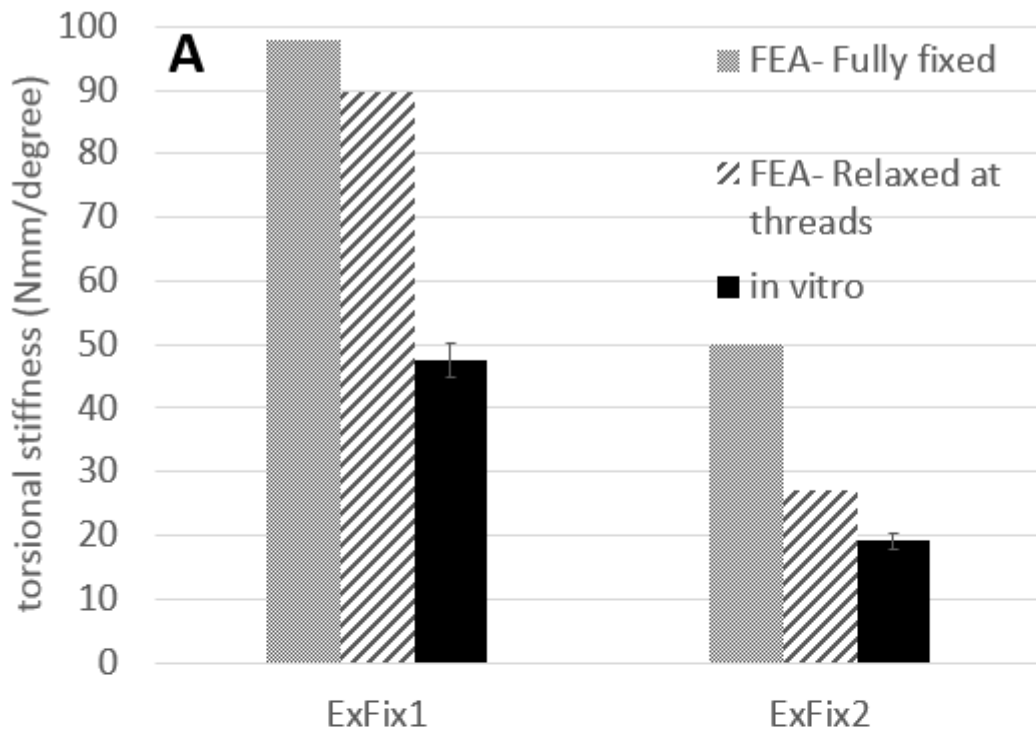


Fig 2

411



412

413

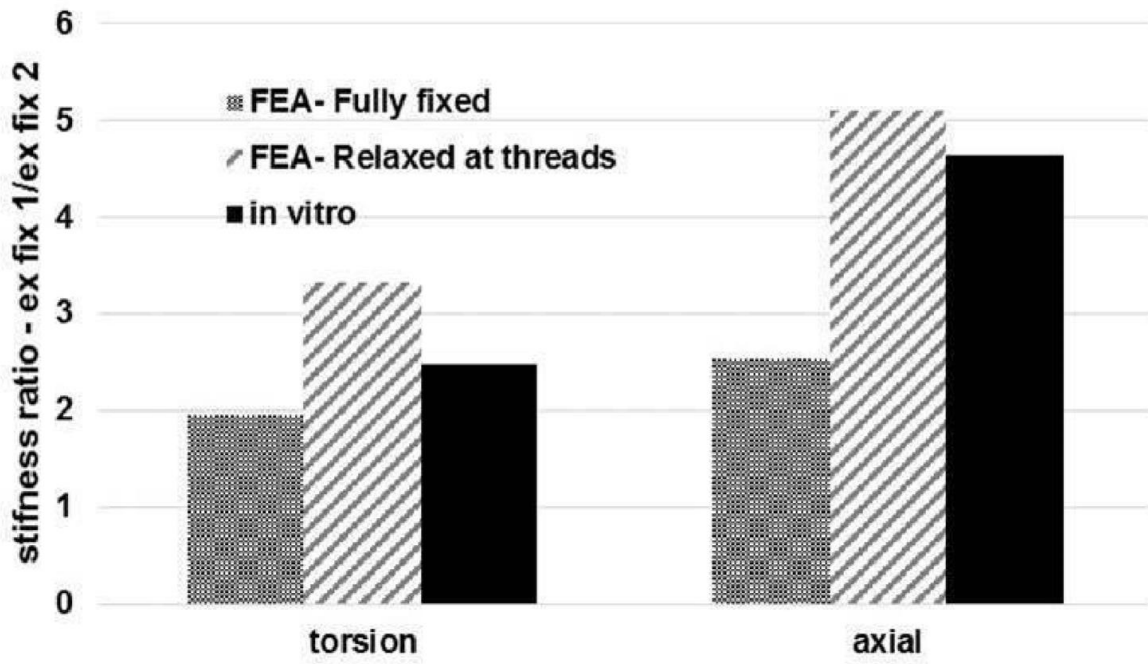
414

415

416

417

418 Fig 3



419

420

421

422

423

424

425

426

427

428

429

430

431

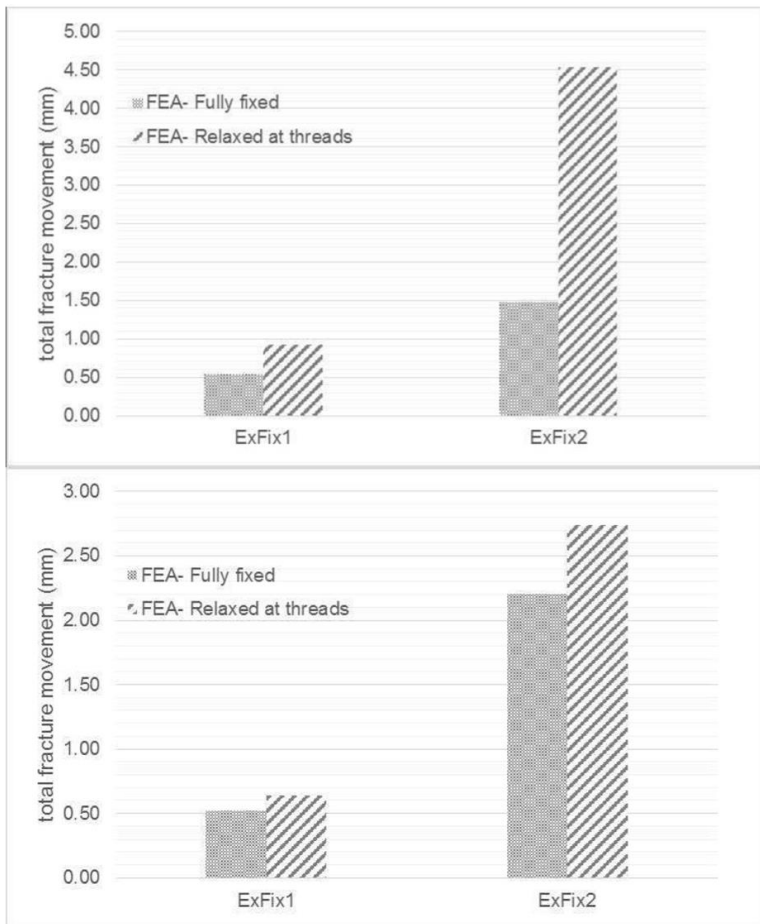
432

433

434

435

436 Fig 4



437

438 Fig 5

439

440

